Noise propagation simulation in and around buildings using improved integral energy equations

Kiyoshi Masuda[1]

[1] Taisei Corporation, Japan

ABSTRACT

If the calculation conditions for noise propagation in and around buildings are perfectly simple, the image-source method or ray-tracing method can be applied. However, conditions in reality are too complicated to apply these methods, because the combination of multiple reflections and diffraction must be taken into account. We have developed an extended integral energy equation method to solve these problems. In the extended integral energy equations, all energy flows between the boundary elements of a calculation model are obtained by solving simultaneous equations that take multiple reflections, multiple diffractions and sound transmission into consideration. To improve the precision of the method, the calculation of first reflections is separated from the calculation of multiple reflections, and the first reflections are calculated by the approximated method derived from the wave theory. This method is applied to the calculation of sounds transmitted through small openings. Predictions using this method corresponded well with measurements from actual sound fields.

Keywords: noise propagation, integral energy equations
I-INCE Classification of Subjects Number(s): 76.1

1. INTRODUCTION

When designing a building, it is important to predict the sound environment in and around the building. An extended integral energy equation method has been developed for precise predictions of noise propagation in and around a multi-room building surrounded by other buildings. In this method, all energy flows between boundary elements of the calculation model are obtained by solving equations considering multiple reflections, multiple diffractions and sound transmission.

To improve the precision of this method, the calculation of first reflections is separated from the calculation of multiple reflections, and the first reflections are calculated using the approximated method derived from wave theory. This method is applied to the calculation of sounds transmitted through small openings.

This paper introduces a theory on improved extended integral energy equations with calculation examples.

2. CALCULATION METHOD

2.1 Extended Integral energy Equations

In extended integral energy equations, all energy flows between the boundary elements of a calculation model are obtained by solving simultaneous equations that take multiple reflections, multiple diffractions and sound transmission into consideration.

In the original integral energy equations method, the directivity of reflection is expressed as a linear combination of specular reflection and random reflection as per Lambert's law (1). Here, it is supposed that only random reflections are dominant and specular reflections are negligible. This supposition saves memory space.

In a sound field surrounded by boundary elements ΔS_i as shown in Figure 1, the incident intensity I_j of the element node j is given by the following integral equation:
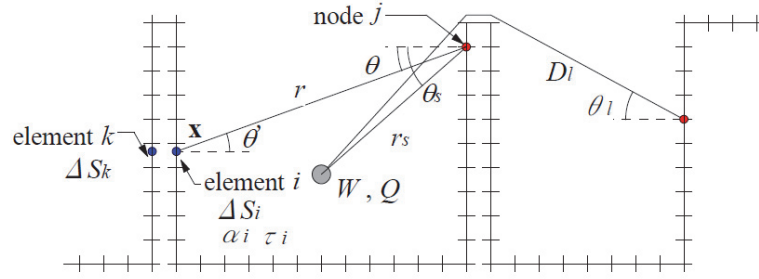
---

[1] Kiyoshi.masuda@sakura.taisei.co.jp

Figure 1 – Extended integral energy equations

$$I_j = \sum_{i=1}^{N}\left[\iint_{\Delta S_i} I(\mathbf{x})\frac{1-\alpha_i}{\pi}\frac{\cos\theta\cos\theta'}{r^2}dS_i\right] + \sum_{k=1}^{N}\left[\iint_{\Delta S_k} I(\mathbf{x})\frac{\tau_i}{\pi}\frac{\cos\theta\cos\theta'}{r^2}dS_k\right]$$
$$+\frac{WQ\cos\theta_s}{4\pi r_s^2} + \sum_{l=1}^{L_{diff}}QD_l\cos\theta_l \tag{1}$$

Where W is the sound power, Q is the directivity index, N is the total number of elements, ΔS_i is the area of the element i, and ΔS_k is the area of element k with the same shape on the back of element i. $I(\mathbf{x})$ is the incident intensity at point $\mathbf{x}$ in an element and approximated by intensities of all nodes in the element using interpolation function.

α_i is the sound absorption coefficient, τ_i is the sound transmission coefficient, θ is the angle of incidence with respect to the normal direction vector of the element containing the node, r is the distance between the node j and point $\mathbf{x}$, r_s is the distance between the node j and the sound source, L_{diff} is the diffraction path number, and D_l is the intensity due to multiple diffraction at the node j in the case where a non-directional sound source is assumed.

By considering the incident intensity of all nodes, we can obtain the integral energy equations. The solutions of these equations give all incident intensities I_i and substituting the solved I_i into Eq. (2), the energy density $E(\mathbf{x}_p)$ at any point in the sound field can be obtained.
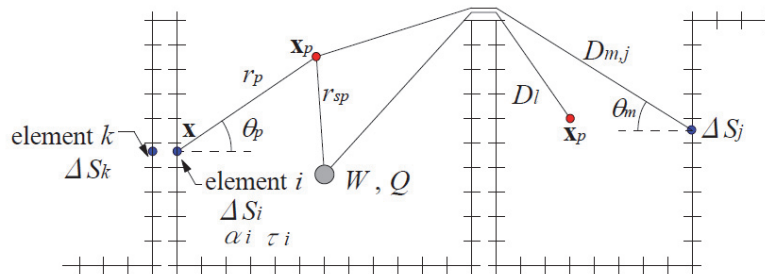

Figure 2 – Energy density calculation at receiving points

$$E(\mathbf{x}_p) = \sum_{i=1}^{N}\left[\iint_{\Delta S_i} I(\mathbf{x})\frac{\cos\theta_p}{r_p^2 c}dS_i\right] + \sum_{j=1}^{N}\left[\sum_{m=1}^{M_{diff}}\frac{D_{m,j}\cos\theta_m}{c}\right] + \sum_{k=1}^{N}\left[\iint_{\Delta S_k} I(\mathbf{x})\frac{\tau_i\cos\theta_p}{r_p^2 c}dS_k\right]$$
$$+\frac{WQ}{4\pi r_{sp}^2 c} + \sum_{l=1}^{L_{diff}}\frac{QD_l}{c} \tag{2}$$

Where c is the sound speed, θ_p is the angle of radiation direction with respect to the normal direction vector of the element, r_p is the distance between the point $\mathbf{x}$ and the receiving point, M_{diff} is the diffraction path number from element i to the receiving point, and $D_{m,j}$ is the intensity due to multiple diffraction at the receiving point in the case where it is assumed to be a non-directional sound source on the element. r_{sp} is the distance between the sound source and the receiving point, L_{diff} is the diffraction path number from the sound source to the receiving point, and D_l is the intensity due to multiple diffractions from the sound source at the receiving point. The calculation

method of the diffraction intensities D_l and $D_{m,i}$ is described in Ref. (2).
The calculation frequency is from the 63 Hz to 4 kHz octave band.

2.2 Improvement of First Reflection Calculation

If there are few reflection surfaces in the sound field, the calculation error increases because Eq. (1) doesn't consider specular reflections. To alleviate this problem, we developed a new method which separates the first reflection calculation from the reflection calculation terms in Eq. (1).

The new integral equation for the incident intensity excluding direct sound intensity I'_j of the element node j is given by Eq. (3).
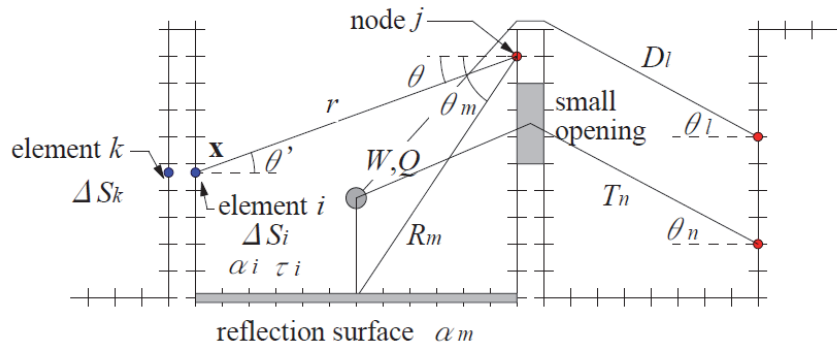

Figure 3 – Improved integral energy equations

$$I'_j = \sum_{i=1}^{N}\left[\iint_{\Delta S_i} I'(\mathbf{x})\frac{1-\alpha_i}{\pi}\frac{\cos\theta\cos\theta'}{r^2}dS_i\right] + \sum_{k=1}^{N}\left[\iint_{\Delta S_k}\left\{I'(\mathbf{x})+\frac{WQ\cos\theta_s}{4\pi r_s^2}\right\}\frac{\tau_i}{\pi}\frac{\cos\theta\cos\theta'}{r^2}dS_k\right]$$
$$+\sum_{m=1}^{M_{ref}}WQR_m(1-\alpha_m)\cos\theta_m + \sum_{l=1}^{L_{diff}}QD_l\cos\theta_l \tag{3}$$

The third term is the first reflection calculation instead of a direct sound calculation in Eq. (1). Here, R_m is the first reflection intensity transfer coefficient of the mth reflection plane calculated by Eq. (4), α_m is the absorption coefficient of the mth reflection surface, and M_{ref} is the total number of reflection planes. The second term calculates the sound transmission of element radiation sound and the direct sound from the source.

R_m is calculated by Eq. (4).

$$R_m = \min\begin{cases} \dfrac{1}{4\pi d_3^2} \\[4mm] \dfrac{1}{4\pi d_3^2}\left(\dfrac{S_m}{\lambda}\left(\dfrac{1}{d_1}+\dfrac{1}{d_2}\right)\right)^2\cos\theta_1\cos\theta_2 \\[4mm] \dfrac{1}{4\pi d_3^2}\left\{10^{-1.9}S_m\left(\dfrac{1}{d_1}+\dfrac{1}{d_2}\right)^2\right\}\left\{1-|\cos\theta_3|\right\}^{\pm 1.3} \\[4mm] \dfrac{1}{4\pi d_3^2}\left\{10f^{-0.8}S_m^{0.4}\left(\dfrac{1}{d_1}+\dfrac{1}{d_2}\right)^2\right\}\left\{1-|\cos\theta_3|\right\}^{\pm 1.3} \end{cases} \tag{4}$$

The fourth equation in Eq. (4) is used when the line from the imaginary source point to the node point crosses the reflection surface as shown in Figure 4. In Eq. (4), $\pm$ assumes a negative value when θ_3 is larger than 90 degrees. S_m is the surface area of the reflection plane, f is frequency, and λ is wavelength. These formulae were derived from parametric study using Helmholtz-Kirchhoff's equation.

Figure 5 shows the reflection sound pressure level distribution calculated using Lambert's law and Eq. (4). The dimension of the reflection surface is 1 meter by 1 meter, and the sound absorption coefficient is zero. The calculation for the 63 Hz octave band is very similar to the random reflection following Lambert's law. The reflection characteristics become more similar to those of specular reflection with increasing frequency.
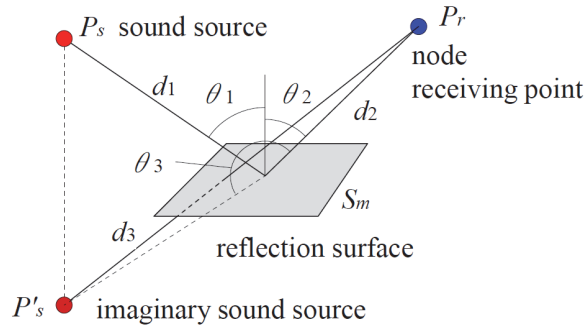
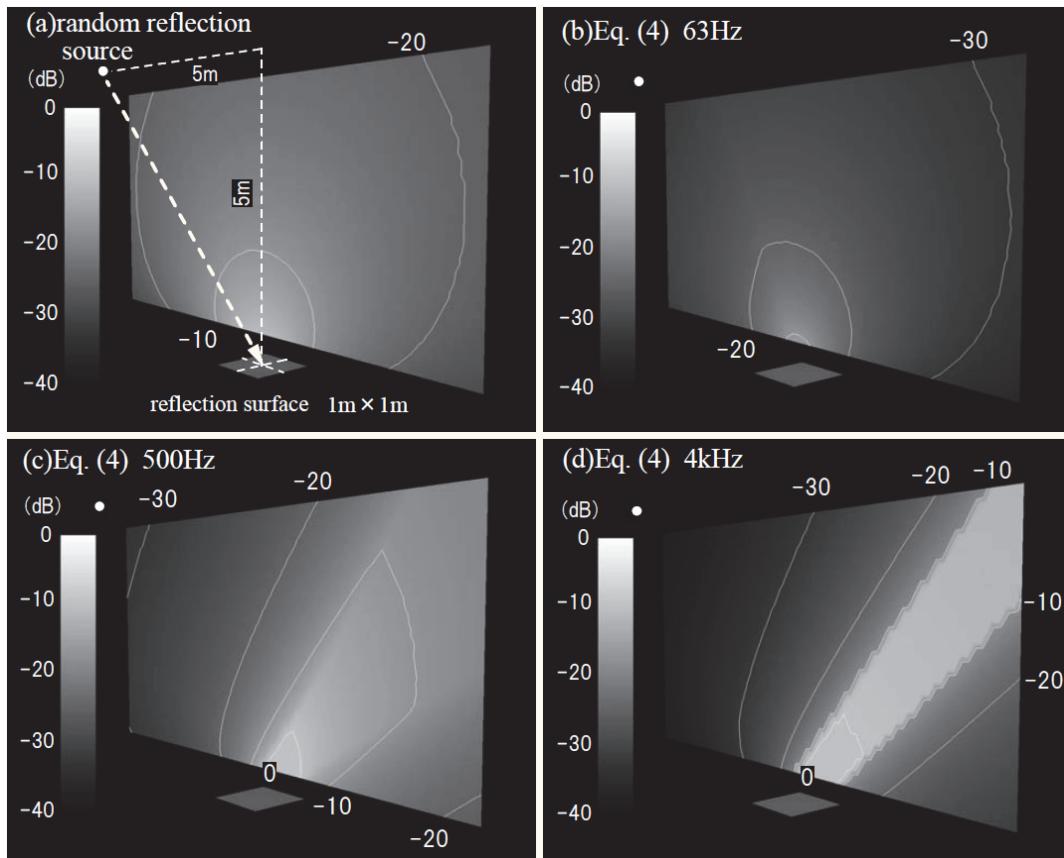Figure 4 – Calculation of first reflection sound

Figure 5 – Sound pressure level distributions calculated using Lambert's law and Eq. (4)

2.3 Improvement of Transmission through Small Opening

If there are small openings in the sound field, the calculation error increases because Eq. (1) doesn't consider the transmission loss of small openings. To alleviate this problem, the calculation method for the first reflection was applied to the calculation of sound transmitted through small openings.

A new integral equation that takes into account transmission through small openings for the incident intensity excluding direct sound intensity I'_j of the element node j is given by Eq. (5).

$$I'_j = \sum_{i=1}^{N}\left[\iint_{\Delta S_i} I'(\mathbf{x})\frac{1-\alpha_i}{\pi}\frac{\cos\theta\cos\theta'}{r^2}dS_i\right] + \sum_{k=1}^{N}\left[\iint_{\Delta S_k}\left\{I'(\mathbf{x})+\frac{WQ\cos\theta_s}{4\pi r_s^2}\right\}\frac{\tau_i}{\pi}\frac{\cos\theta\cos\theta'}{r^2}dS_k\right]$$
$$+ \sum_{m=1}^{M_{ref}}WQR_m(1-\alpha_m)\cos\theta_m + \sum_{l=1}^{L_{diff}}QD_l\cos\theta_l + \sum_{n=1}^{N_{trs}}WQT_n\cos\theta_n$$

(5)

Where T_n is the small opening transmission intensity transfer coefficient of the nth small opening calculated by Eq. (6), and N_{trs} is the total number of small openings.
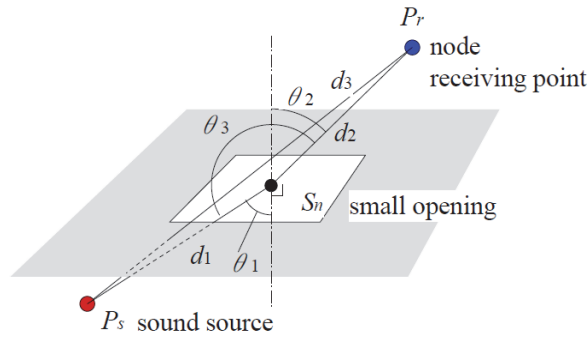
Figure 6 – Calculation of small opening transmission sound

$$T_n = \min \begin{cases} \dfrac{1}{4\pi d_3{}^2} \\[2mm] \dfrac{1}{4\pi d_3{}^2} \left(\dfrac{S_m}{\lambda}\left(\dfrac{1}{d_1}+\dfrac{1}{d_2}\right) \right)^2 \cos\theta_1 \cos\theta_2 \\[3mm] \dfrac{1}{4\pi d_3{}^2} \left\{ 10^{-1.9} S_n \left(\dfrac{1}{d_1}+\dfrac{1}{d_2}\right)^2 \right\} \left\{ 1-|\cos\theta_3| \right\}^{\pm 1.3} \\[3mm] \dfrac{1}{4\pi d_3{}^2} \left\{ 10 f^{-0.8} S_m{}^{0.4} \left(\dfrac{1}{d_1}+\dfrac{1}{d_2}\right)^2 \right\} \left\{ 1-|\cos\theta_3| \right\}^{\pm 1.3} \end{cases} \tag{6}$$

The fourth equation in Eq. (6) is used when the line from the source point to the node point crosses the small openings as shown in Figure 6. In Eq. (6), $\pm$ assumes a negative value when θ_3 is larger than 90 degrees.

By considering the incident intensity of all nodes, we can obtain the improved integral energy equations. Solving these equations gives all incident intensities I_i, and by substituting the solved I_i into Eq. (7), the energy density $E(\mathbf{x}_p)$ at any point in the sound field can be obtained.
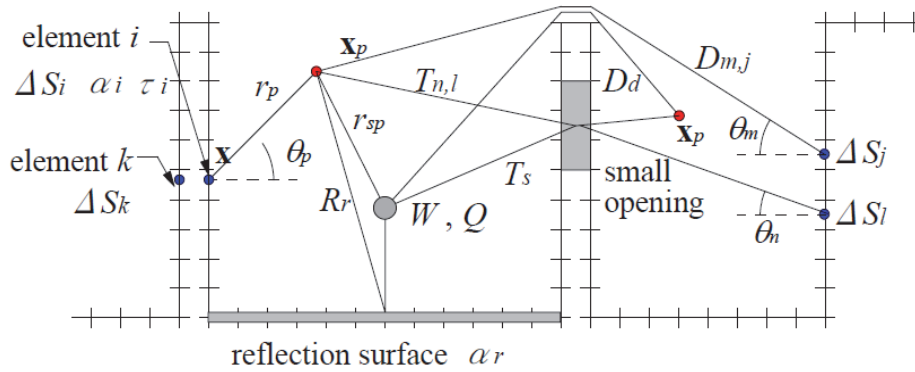

Figure 7 – Energy density calculation at receiving points using the improved method

$$E(\mathbf{x}_p) = \sum_{i=1}^{N}\left[\iint_{\Delta S_i} I(\mathbf{x})\frac{\cos\theta_p}{r_p{}^2 c}dS_i \right] + \sum_{i=1}^{N}\left[\sum_{m=1}^{M_{diff}}\frac{D_{m,i}\cos\theta_m}{c} \right] + \sum_{k=1}^{N}\left[\iint_{\Delta S_k} I(\mathbf{x})\frac{\tau_i \cos\theta_p}{r_p{}^2 c}dS_k \right]$$
$$+ \sum_{i=1}^{N}\left[\sum_{n=1}^{M_{trs}}\frac{T_{n,i}\cos\theta_n}{c} \right] + \frac{WQ}{4\pi r_{sp}{}^2 c} + \sum_{r=1}^{S_{ref}}\frac{WQR_r(1-\alpha_r)}{c} + \sum_{d=1}^{S_{diff}}\frac{QD_d}{c} + \sum_{s=1}^{S_{trs}}\frac{WQT_s}{c} \tag{7}$$

Where M_{trs} is the transmission path number from element i to the receiving point through small openings, and $T_{n,i}$ is the intensity due to transmission through a small opening at the receiving point in the case where it is assumed to be a non-directional sound source on the element. S_{ref}, S_{diff}, S_{trs} are the path numbers from the sound source to the receiving point, and R_r, D_d, T_t are the reflection, diffraction, and transmission intensity transfer coefficients.

3. EXPERIMENT

3.1 Improved Calculation of First Reflection

In order to confirm the accuracy of the new first reflection calculation method, a noise propagation experiment was conducted in an actual sound field, as shown in Figure 8. A 3-D calculation model is shown in Figure 8.
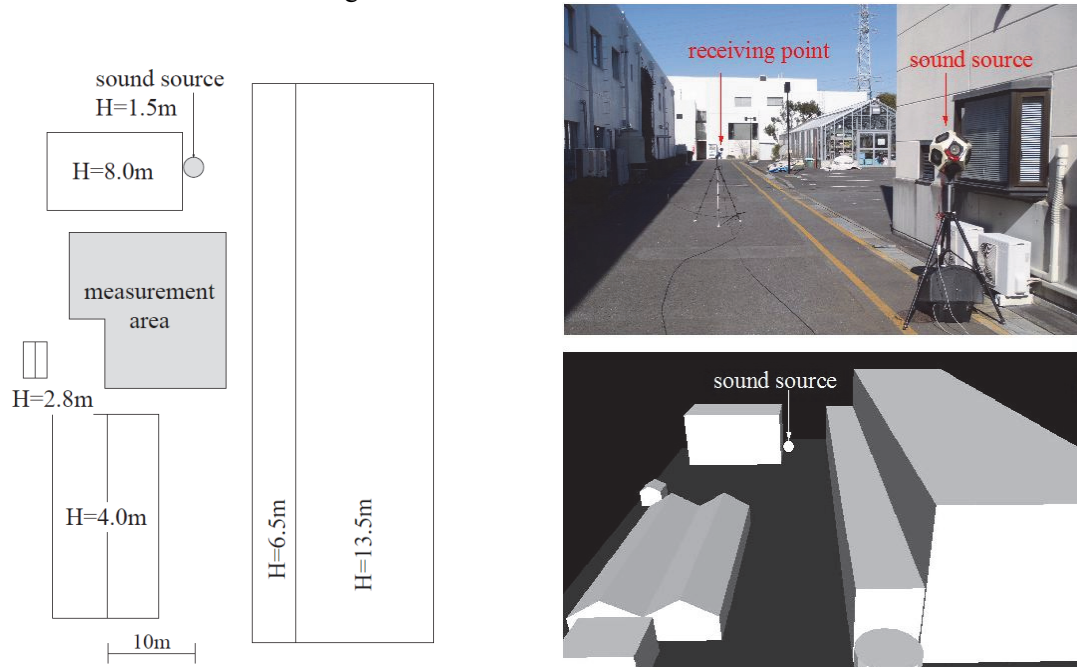

Figure 8 – Experiment for improved calculation of first reflection

The sound source was a dodecahedron speaker which radiated random broadband noise. The receiving points were set every two meters in the measurement area shown in Figure 8 and the noise levels were measured. The power level of the sound source was estimated by the sound pressure levels at measurement points near the sound source.

The measured and calculated relative noise level distributions are shown in Figure 9.

The calculation using the old method which calculates only random reflections ((b) in Figure 9) demonstrated good correlation with the actual measurements, but the calculation using the new method, which separates off the first reflection calculation ((c) in Figure 9), demonstrated better correlation in measurement areas further from the source point.
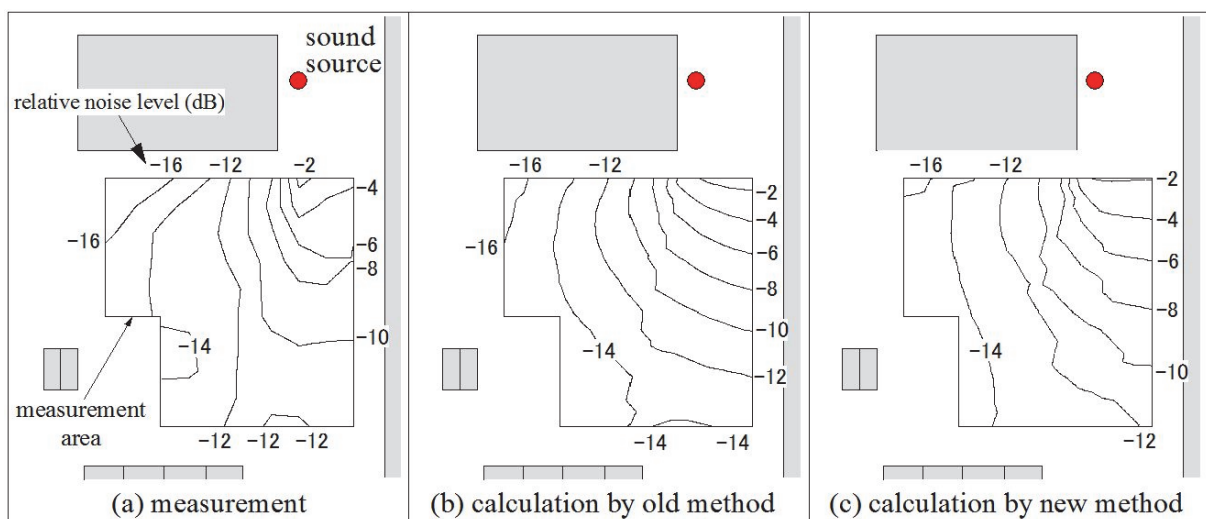

Figure 9 – Experimental results for improved calculation of first reflection

3.2   Improved Calculation of Transmission through Small Opening

In order to confirm the accuracy of the new small openings transmission method, a noise propagation experiment was conducted in an actual sound field, as shown in Figure 10. A 3-D calculation model is shown in Figure 10.
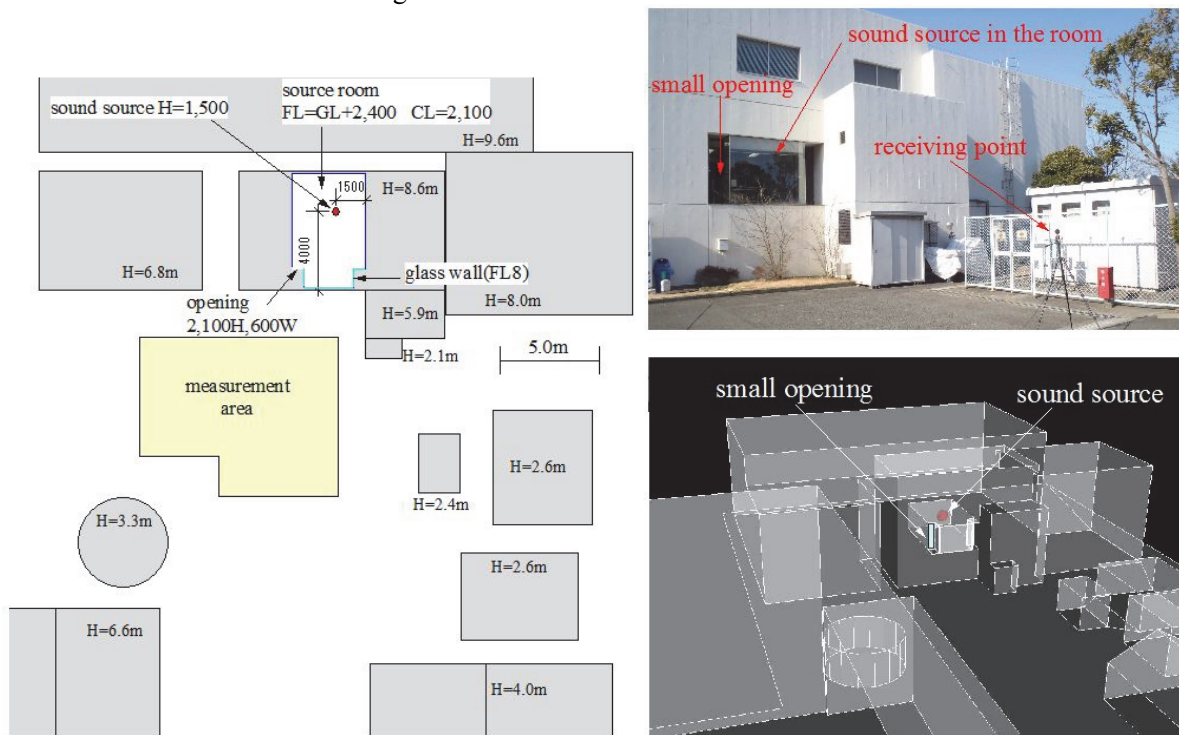

Figure 10 – Experiment for improved calculation of transmission through a small opening

The sound source was a dodecahedron speaker which radiated random broadband noise in the source room within a building. The random noise was transmitted through the small opening and the outer glass wall, and propagated around the buildings. The receiving points were set every two meters in the measurement area shown in Figure 10, and the noise levels were measured.

The measured and calculated relative noise level distributions are shown in Figure 11.

In the old method calculation, the small opening is set as a wall whose transmission loss is 0 dB. The calculation using the old method is 3 to 6 dB higher than the actual measurement ((b) in Figure 11), but the calculation using the new method, which considers transmission through the small opening ((c) in Figure 11), demonstrates better correlation with the actual measurement.
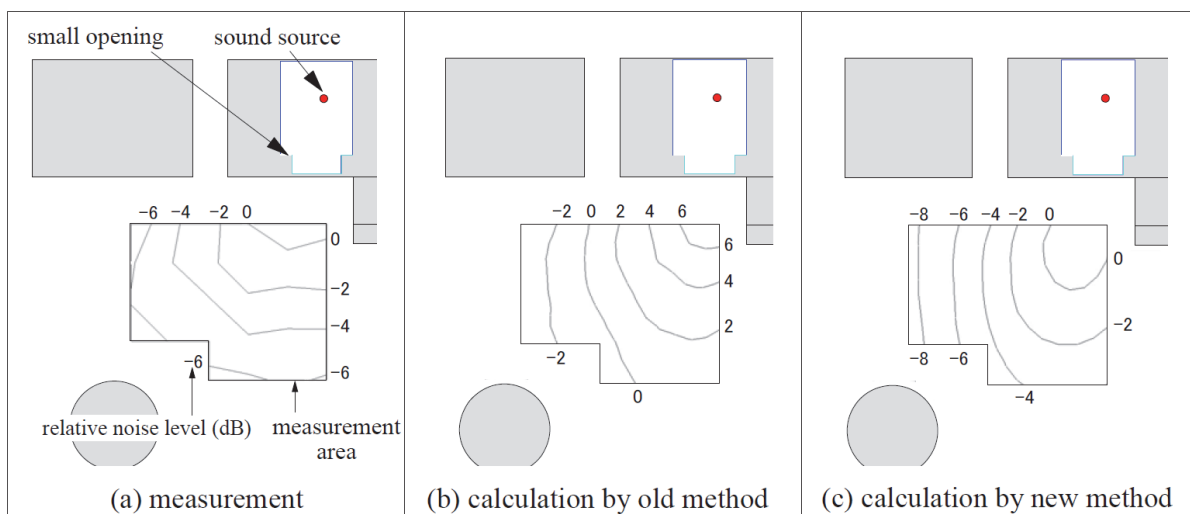

(a) measurement   (b) calculation by old method   (c) calculation by new method

Figure 11 – Experimental results for improved calculation of transmission through a small opening

4. CONCLUSIONS

To improve the precision of the extended integral energy equations method, the calculation of first reflections is separated from the calculation of multiple reflections, with the first reflections being calculated using the approximated method derived from wave theory. This method was applied to the calculation of sound transmitted through small openings.

Predictions using this method corresponded better with the measurements from actual sound fields than the former method.

REFERENCES

1. Kuttruff H, Simulierte Nachschallkurven in Rechteckraeumen mit diffusem Schallfeld, Acustica, 25, 1971, 333-342.
2. Masuda K, Sound environment simulation system for prediction of noise propagation in and around buildings, ASVA97 proceedings, 1997, 585-590.